Journal of Alloys and Compounds 634 (2015) 1–5

Contents lists available at ScienceDirect

Journal of Alloys and Compounds

journal homepage: www.elsevier.com/locate/jalcom

Thermoelectric properties of A-site substituted Lanthanide $Ca_{0.75}R_{0.25}MnO_3$

X.H. Zhang, J.C. Li *, Y.L. Du, F.N. Wang, H.Z. Liu, Y.H. Zhu, J. Liu, W.B. Su, C.L. Wang, L.M. Mei

School of Physics, Shandong University, Jinan 250100, P.R. China

ARTICLE INFO

Article history:
Received 3 December 2014
Received in revised form 31 January 2015
Accepted 10 February 2015
Available online 16 February 2015

Keywords:
$CaMnO_3$
First principle calculation
Lanthanide doping
Thermoelectric properties

ABSTRACT

We present the electronic structure and thermoelectric properties of doped and intrinsic $CaMnO_3$ investigated by first principles and semi-classic Boltzmann theory. The G-type anti-ferromagnetic phase is most stable among five intrinsic anti-ferromagnetic phases, however, the C-type phase is most stable phase after Lanthanides doping in A-site of $CaMnO_3$. Electrons transfer from Lanthanides to Mn *d* orbital in 25% Lanthanides doped materials, which result in part of conductive bands are occupied by Mn *d* electrons. The electron transport changes from semiconductor (intrinsic) to metal (doped), this change can be found in Seebeck coefficient and electrical conductivity as the function of temperature. The electrical conductivity is enhanced by Lanthanides doping, and about 2 orders of magnitudes higher than those of intrinsic $CaMnO_3$. So the Lanthanides doping is useful method to modify thermoelectric properties of $CaMnO_3$.

1. Introduction

Thermoelectric (TE) materials which can convert heat energy into electrical energy directly have attracted a wide range of interests. In recent years, more and more attentions are focus on oxide thermoelectric materials, such as layered perovskite $Ca_3Co_4O_9$ [1–4], electronic doped $CaMnO_3$ [5–10], and electronic doped Ti oxide [11–14], because they are more suitable for high temperature application in respect that their structural and chemical stability, low cost and so on. The efficiency of a TE generator depends on the material's TE dimensionless figure of merit (ZT). The ZT is defined as $ZT = S^2\sigma T/\kappa$, where S is Seebeck coefficient, σ is electrical conductivity, κ is total thermal conductivity and T is absolute temperature respectively. Thermoelectric materials of $CaMnO_3$ has high Seebeck coefficient [15,16], however the value of ZT is low because of low electrical conductivity [16]. So more and more efforts are focus on improving their electrical conductivity by n-type doping.

So far, Ca site doping [8,17], Mn site doping [10,18,19] and double sites doping [20,21] for $CaMnO_3$ has been done to modify the TE property in order to improve the dimensionless figure of merit ZT value. Experimentally [22,23], it is found that doping at Ca site of $CaMnO_3$ lead to enhancement of thermoelectric properties. A metal–insulator transition is induced by doping Tb, Ho and Y in $CaMnO_3$ [22]. The doping of Yb, Tb, Nd, and Ho in $CaMnO_3$ improved the value of ZT (0.16 at 1000 K for $Ca_{0.9}Yb_{0.1}MnO_3$) [23]. For the $CaMnO_3$ substituted by the trivalent elements at Ca site, the electrical conductivity σ are increased obviously, along with a moderate decrease in the absolute value of the Seebeck coefficient S for $Ca_{0.9}Bi_{0.1}MnO_3$ [24]. Wang et al. [25–29] studied all Lanthanide elements substitution, reported the high temperature transport and thermoelectric properties of $Ca_{1-x}R_xMnO_3$. The resistivity and the absolute value of the Seebeck coefficient S were decreased and the thermoelectric figure of merit ZT for $Ca_{1-x}R_xMnO_3$ reached 0.2 at 1000 k. It indicates that Lanthanides doping at Ca site is more effective than that of other elements in improving TE properties of $CaMnO_3$. However, the origin of the improvement is still not clear. Several theoretical studies have been focused on analyzing the physical property of $CaMnO_3$. Zhang et al. investigated the electronic structure of G-type anti-ferromagnetic $CaMnO_3$ using DFT theory based on generalized gradient approximations (GGA), and found an indirect band gap of 0.7 eV [30], which implies its semiconductor feature. The thermoelectric and transport effect of Na, Ga, and Sr doping are investigated in detail, a semiconductor-to-conductor transition are predicted in the doped systems, and the thermoelectric properties are improved [31,32]. Based on the electronic structure, it is noted that the enhancement of ZT results from the improvement of the Seebeck coefficient, carrier conduction capability and restrained phonon conduction. So far, the $CaMnO_3$ doped with rare earth elements are investigated detailed in experiments [33,34], however,

---

* Corresponding author.
E-mail address: lijichao@sdu.edu.cn (J.C. Li).

http://dx.doi.org/10.1016/j.jallcom.2015.02.074

the theoretical investigation of underlying mechanisms of enhancement of ZT are still lacked. In this work, the electronic structures are calculated using the first principles method for the $CaMnO_3$ doped by 25% Lanthanides at Ca-site. We predict the thermoelectric properties effect of Lanthanide doping, and find that the electron transfer from Lanthanide elements to Mn result in the enhancement of electrical conductivity by doping Lanthanides. Based on electronic structures, we explain the underlying mechanism of electronic transport change from semiconductor to metallic feature, which caused by Lanthanides doping.

2. Computational details

The crystal structure of perovskite type $CaMnO_3$ is orthorhombic symmetry. The cell parameters is described as $a = 5.2812$, $b = 7.4571$, $c = 5.2753$, $\alpha = \beta = \gamma = 90°$. The atomic fractional coordinates used in our calculations are same with Ref. [30]. The $CaMnO_3$ is an anti-ferromagnetic material, there exist five magnetic phases, A-type, C-type, E-type, G-type and C–E-type anti-ferromagnetism. We optimized the unit cell with formula $Ca_4Mn_4O_{12}$ in different magnetic phase, and find the total energy of G-type anti-ferromagnetism is the lowest among five phases, this indicates that the G-type phase is the most stable. Thus our calculation was based on the G-type anti-ferromagnetic $CaMnO_3$ with a space of p_{nma}. All the Lanthanides are chosen to dope in G-type anti-ferromagnetic (G-AFM), the formula of the doping cell is $Ca_{0.75}R_{0.25}MnO_3$ (R is Lanthanide).

Calculations with the ultra-soft pseudo-potential plane wave method and generalized gradient approximations (GGA) based on DFT theory is performed using the Vienna Ab-initio Simulation Package (VASP). Pseudo atomic calculation for Ca_pv, Mn and O is performed, and Lanthanide all use the same Core = Xe^4. The valence electronic wave functions are expanded in a plane-wave basis set up to an energy cutoff of 400 eV. Total energy calculation convergence criteria for 1×10^{-4} eV, ion relaxation convergence criteria for all the forces between the atoms is less than 1×10^{-2} eV/Å. The atom positions were allowed to be optimized during the geometric optimization. In the total energy calculations, integrations over the Brillouin zone are performed for the unit cell. In the electronic structure calculation, Brillouin zone is sampled with a $5 \times 3 \times 5$ k-point grid; the band energy tolerance was set as 0.01 meV.

Based on electronic structure, the thermoelectric properties are calculated using semi-classical Boltzmann theory and the rigid band approach by analyzing the band structure. BoltzTraP is a program for calculating the semi-classic electrical transport coefficients. It is based on a smoothed Fourier interpolation of the bands. From this analytical representation we calculate the derivatives necessary for the transport distributions. The electrical conductivity can be calculation as a function of temperature as

$$\sigma_{\alpha\beta}(T,\mu) = \frac{1}{\Omega}\int \sigma_{\alpha\beta}(\varepsilon)\left[-\frac{\partial f_{\mu}(T,\varepsilon)}{\partial \varepsilon}\right]d\varepsilon \qquad (1)$$

where the f represents the Fermi distribution function, the T is the absolute temperature, the μ is the chemical potential and the Ω is the volume. The functions can thereafter be calculated from the band structure results except for the relaxation time τ. Theoretically, the relaxation time term τ is correlated with crystal structure, temperature as well doping content, microstructure and texture of specific materials. In the present we will use the simplest approximation for the relaxation time, namely to keep it constant, which is the most often used in praxis [35,36].

Under the constant relaxation time approximation, the Seebeck coefficient can be formulated by

$$S = \pm\frac{1}{eT}\left[E_F - \int_0^{\infty} g(E)\tau E^2 \frac{df_0(E)}{dE}dE \Big/ \int_0^{\infty} g(E)\tau E \frac{df_0(E)}{dE}dE\right] \qquad (2)$$

where e is the charge of the electron, E_F is Fermi level, $g(E)$ is density of state, τ is relaxation time. Here we also treat τ as a constant. The Fermi level E_F and the density of state $g(E)$ as a function of E can be obtained from the DFT calculation, thus the Seebeck coefficient as a function of temperature T can be determined. The original k mesh of the BoltzTraP was interpolated onto a mesh four times denser than the original.

3. Results and discussion

The total energy of the five phases of $CaMnO_3$ are calculated to find the most stable phase among the five phases, it is noted that the G-AFM is the most stable phase among the five phases. Our calculations are in good agreement with previous one [30]. For the G-AFM phase, the band structure are obtained by GGA and shown in Fig. 1(a). It is noted that the indirect band gap is 0.7 eV, and the valence bands near the Fermi level are composed of Mn d and O p electrons, our calculations are in agreement with previous calculations [30,31], and imply the G-AFM phase is semiconductor, which can explain the experiments [37].

For the intrinsic G-AFM $CaMnO_3$, there are two doping site, Ca-site and Mn-site. The Lanthanides are doped in the two sites, the binding energy of different doping are calculated, and listed in Table 1. Comparing the binding energy of two positions doping, it is easy to find that Ca-site doping is more stable than Mn-site doping. Our calculations explain the previous experiments [7,38,39,23,40–43]. For the $CaMnO_3$ with Lanthanides 25% doping,

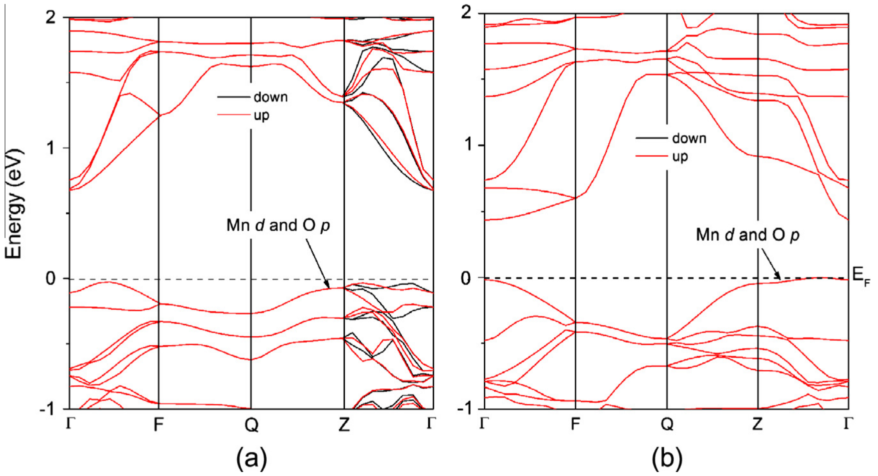

Fig. 1. The energy band structure of G-AFM phase and C-AFM phase of $CaMnO_3$. (a) G-AFM phase and (b) C-AFM phase.

Table 1
The binding energy (eV) of C-AFM $CaMnO_3$ doped with Lanthanide elements in Ca-site and Mn-site.

	La	Ce	Pr	Nd	Pm	Sm	Gd	Tb	Dy	Ho	Er	Tm	Lu
Ca	−4.71	−4.45	−4.45	−6.24	−4.60	−4.61	−4.75	−4.77	−4.76	−4.76	−4.76	−4.77	−4.75
Mn	1.52	−1.27	3.19	0.94	−0.98	2.64	1.07	−2.59	−2.73	−2.29	0.40	0.98	1.01